



**HAL**  
open science

# Solid and Non-Solid Dielectric Material Characterization for Millimeter and Sub-Millimeter Wave Applications

Daniel Bourreau, Alain Peden

► **To cite this version:**

Daniel Bourreau, Alain Peden. Solid and Non-Solid Dielectric Material Characterization for Millimeter and Sub-Millimeter Wave Applications. EuMC 2020: 50th European Microwave Conference, Jan 2021, Utrecht, Netherlands. pp.909-912, 10.23919/EuMC48046.2021.9338045 . hal-03421606

**HAL Id: hal-03421606**

**<https://hal.science/hal-03421606>**

Submitted on 5 Jul 2023

**HAL** is a multi-disciplinary open access archive for the deposit and dissemination of scientific research documents, whether they are published or not. The documents may come from teaching and research institutions in France or abroad, or from public or private research centers.

L'archive ouverte pluridisciplinaire **HAL**, est destinée au dépôt et à la diffusion de documents scientifiques de niveau recherche, publiés ou non, émanant des établissements d'enseignement et de recherche français ou étrangers, des laboratoires publics ou privés.

# Solid and Non-Solid Dielectric Material Characterization for Millimeter and Sub-Millimeter Wave Applications

Daniel Bourreau, Alain Pédén

Lab-STICC, UMR 6285 CNRS, IMT Atlantique, Brest, France

{daniel.bourreau, alain.peden}@imt-atlantique.fr

**Abstract** — An accurate quasi-optical S-parameter measurement method implemented in the normalized frequency bands Ka, W and J is presented in this paper. Permittivity extraction of various solid or non-solid dielectric materials is performed using the 4 S-parameters without time domain gating nor filtering. The procedure is validated through the comparison between the simulated and measured 4 S-parameters in magnitude and phase. Results are given for the Rexolite over a wide frequency span from the Ka to J band while some non-solid materials were characterized in the W band. Moreover, effects of rain flow on a dielectric slab were investigated for automotive radar applications in the W band and preliminary results are given.

**Keywords** — characterization, free space, dielectric permittivity, solid and non-solid material, rainfall, car bumper.

## I. INTRODUCTION

Millimeter waves up to THz are increasingly being used or foreseen in various applications such as 5G (backhaul), RFID tags to analyze the risks associated with aging structures, imaging for non-destructive control and security, automotive radars, radiometry,... Knowledge of the complex dielectric permittivity of materials is essential to achieve the specifications in the design of devices and systems at very high frequencies. Moreover, the study of the propagation and the interactions of waves with the environment also requires a detailed knowledge of these characteristics. Material characterization can be performed in a rectangular or coaxial waveguide, or in a cavity, where machined samples are inserted. Due to very small dimensions of the waveguides at millimeter waves and very small frequency bandwidth extraction in cavities, free space non-resonant techniques are preferred at very high frequencies [1].

This paper presents a technique and the associated setups for the measurement of the 4 S-parameters of dielectric slabs in the millimeter wave range. The technique is based on free space measurements and is implemented in the Ka (26-40 GHz), W (75-110 GHz) and J (220-330 GHz) normalized frequency bands. The 4 S-parameters over each frequency band are used to extract the complex permittivity of solid materials [2]–[4], while non-solid materials such as water or sand are measured using a pre-characterized container [5]–[7]. As an extend to this work, the impact of rain on a car bumper is also investigated in

the W band [8] and preliminary results of wet radome modeling are presented.

## II. TEST BENCH DESCRIPTION

The quasi-optical technique is based on “free space” propagation between two antennas placed opposite to each other. A material under test (MUT) with large dimensions, located between them, interacts with the electromagnetic beam and the consequent perturbations characterize the transmission and reflection coefficients, that is, the S-parameters of the MUT. Specific antennas, using a horn and a lens, are designed to create a focused or paraxial gaussian beam, depending on the ratio between the waist  $W_0$  and wavelength  $\lambda$  [9]. The higher the ratio, the more paraxial the beam. A highly paraxial beam is preferred so that the MUT position is not critical and S-parameters can be measured without filtering nor time gating. Therefore, the waist is the optimal position for the free space S-parameter measurement of a device under test such as dielectric slab, frequencies selective surfaces, polarizer, etc. (see Fig. 1).

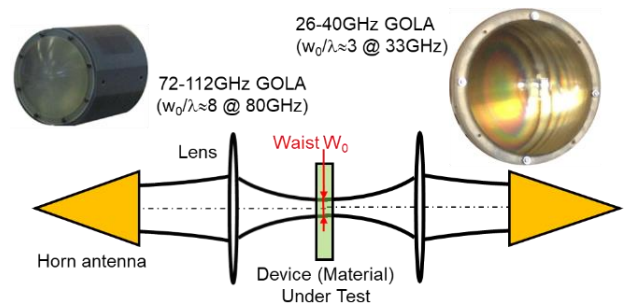


Fig. 1. Gaussian beam focused to obtain the waist

The test bench in the W band was developed using purchased GOLA (Gaussian Optics Lens Antenna) with  $W_0/\lambda \approx 8$  and validated through various experimental results. In the Ka band, specific corrugated horns were designed to create a gaussian beam with a  $W_0/\lambda$  ratio of about 3. The in-house measurement setup in the J band uses commercial horns and lens with  $W_0/\lambda \approx 13$ . Lastly, the D band (110-170 GHz) test bench is now under study. As depicted in Fig. 2, the material is easily placed on a motorized mount between the GOLA

antennas and measurements on normal incidence can be carried out as well as with an incidence angle if needed.

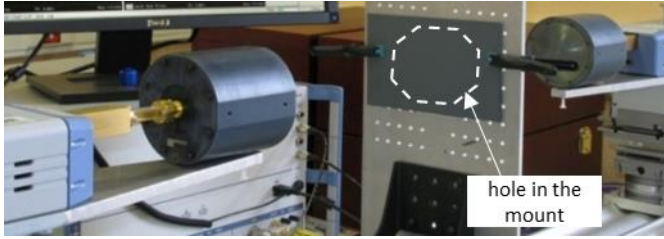


Fig. 2. Quasi-optical test bench in the W band with a PVC slab under test. A hole, hidden by the slab, is made in the mount (see also Fig. 10).

The 4 S-parameter measurement requires a full 2-port calibration of the setup. Therefore, a free space Thru-Reflect-Line (TRL) technique is used to ensure an accurate location of the reference plane, as proposed in [3] using the W band setup. The described calibration procedure is applied in the same way for the Ka, D and J test benches: a metal plate is used for the reflect standard, the line is achieved by moving away one of the two antennas by a distance of around a quarter wavelength at the center frequency and the thru by moving back the shifted antenna.

### III. DIELECTRIC PERMITTIVITY CHARACTERIZATION

#### A. Solid material characterization

The permittivity extraction is carried out using the analytical model of a dielectric slab whose parallel faces are under normal incidence of a plane wave (see Fig. 3). As the slab thickness is measured with a caliper, the relative complex permittivity  $\epsilon_r = \epsilon'_r + j\epsilon''_r$  can be extracted at each frequency point only from the measured  $S_{12}$  or/and  $S_{21}$  parameters (magnitude and phase) by minimization of an error function.

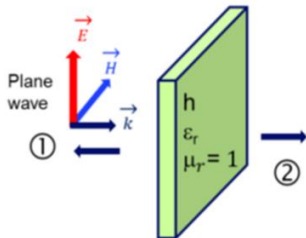


Fig. 3. Slab model under plane wave incidence

Using the extracted value of the permittivity, the  $S_{11}$  and  $S_{22}$  coefficients are then used to refine, with some iterations, the slab thickness  $h$  by comparing the measured and simulated S-parameters.

As an example, the permittivity extraction result for a 12.815 mm Rexolite slab is given in Fig. 4 for the 3 normalized frequency bands, from 26.5 up to 330 GHz.

To validate the permittivity extraction in the J band, using the mean values, the comparison between the simulated and measured transmission and reflection coefficients in magnitude and phase is performed. As depicted in Fig. 5 and Fig. 6, very good agreement is obtained with no preliminary filtering or time domain gating applied to the calibrated S-parameters.

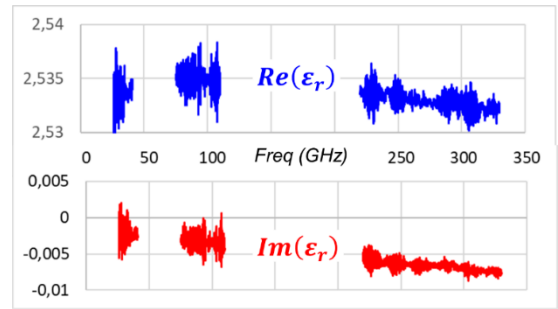


Fig. 4. Extracted permittivity (real and imaginary parts) of a Rexolite slab

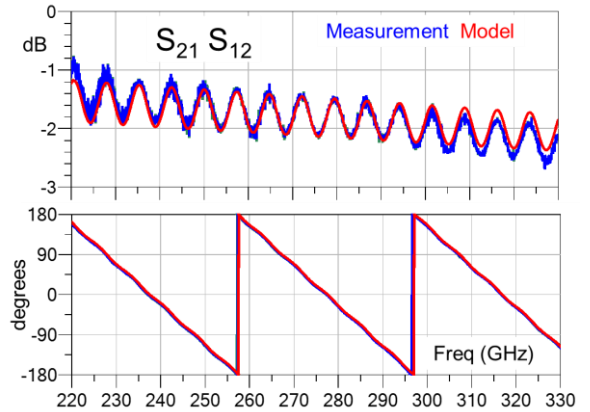


Fig. 5. Comparison between measured and simulated  $S_{21}$  and  $S_{12}$  parameters (magnitude and phase) of a Rexolite slab

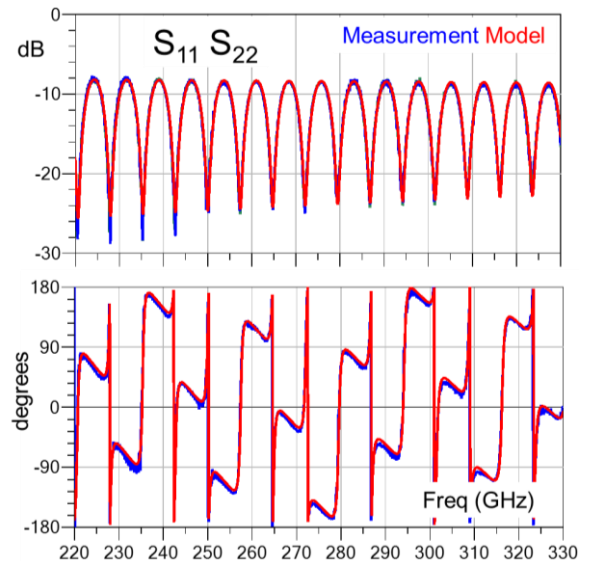


Fig. 6. Comparison between measured and simulated  $S_{11}$  and  $S_{22}$  parameters (magnitude and phase) of a Rexolite slab

#### B. Non-solid material characterization

In order to characterize a non-solid material, a specific container (using anti-leak seal for liquids) made up of two dielectric parts was designed [10]. The internal transverse dimensions of the container depend on the operating frequency and more particularly on the size of the electromagnetic beam. In the W band, a square about 10 x 10 cm<sup>2</sup> is used. In the Ka band, a square about 22 x 22 cm<sup>2</sup> is used.

Using the extracted value of the permittivity, the  $S_{11}$  and  $S_{22}$  coefficients are then used to refine, with some iterations, the slab thickness by comparing the measured and simulated S-parameters. To model the container, a cascade of 3 plates (namely A, M and B) can be considered, according to Fig. 7.

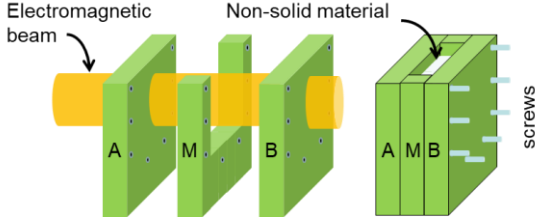


Fig. 7. Container assembly for non-solid material characterization

The dielectric slabs A and B (PVC) are separately pre-characterized. Therefore, the complex permittivity and thickness of each part (A, B) of the container are known:  $\epsilon_{rA}$ ,  $h_A$ ,  $\epsilon_{rB}$  and  $h_B$ . The S-parameter measurement of the assembly makes it possible to retrieve the characteristics of the unknown material ( $\epsilon_{rM}$ ,  $h_M$ ). The approach uses the transfer (T) matrix transformation which leads to:

$$[T_{AMB}] = [T_A^{model}] \cdot [T_M^{model}] \cdot [T_B^{model}] \quad (1)$$

where the transfer matrix  $T_{AMB}$  is calculated from the measured S-parameters of the assembly and  $T^{model}$  is the calculated T-matrix of each A, B and M slab [10].

The measured value  $h_M$  is taken as an initial value of the material thickness and it is slightly adjusted by a few iterations.

As an example, the water permittivity extracted by this procedure is compared with the single-Debye model (see Fig. 8). Moreover, as seen in Fig. 9, very good agreement between the simulated and measured S-parameters is obtained with no filtering or time domain gating applied to the measured data.

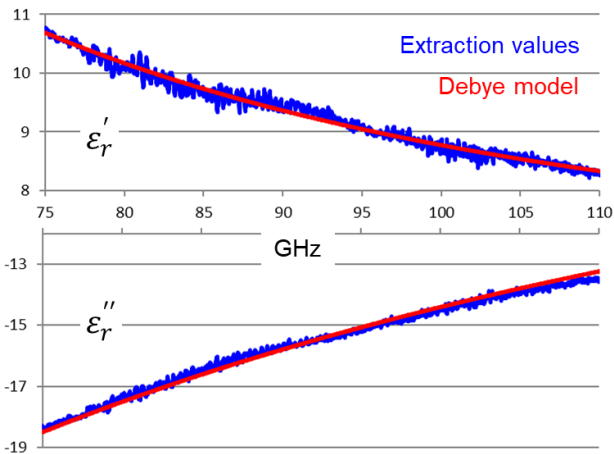


Fig. 8. Water complex permittivity extraction in the W band

The discrepancy observed between the simulated and the measured S-parameters comes from a non-perfect parallelism of the 3 cascaded slabs of the container. This imperfection has less impact on the transmission coefficient.

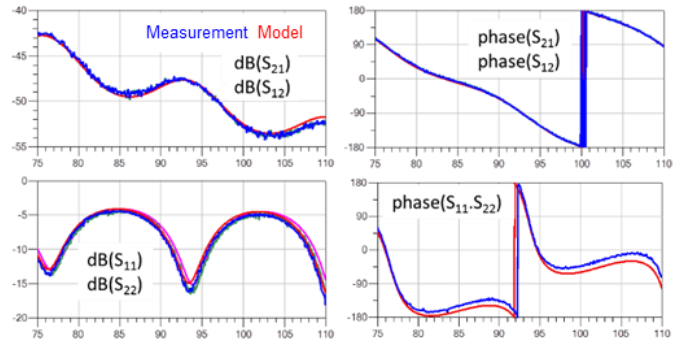


Fig. 9. Comparison of the S-parameters of the container filled with water

#### IV. EFFECT OF WATER ON A DIELECTRIC SLAB

##### A. Test bench

Experimentations on wet materials were performed in the W and Ka bands using the previously described setups (see Fig. 2). This study is of great interest for automotive applications as the performances of the radar placed behind the car bumper are impaired by rain [11], [12].

Water drops were sprayed on one side of the material as well as water flowing, as depicted on Fig. 10, with various drop sizes and densities on the surface. Even if the amount of sprayed water and the water quantity over the surface of the material is not perfectly controlled, this simple test gives some interesting preliminary results about the impact of water on the reflection and transmission coefficients. Investigations carried out for water flow modelling are described in the next section.

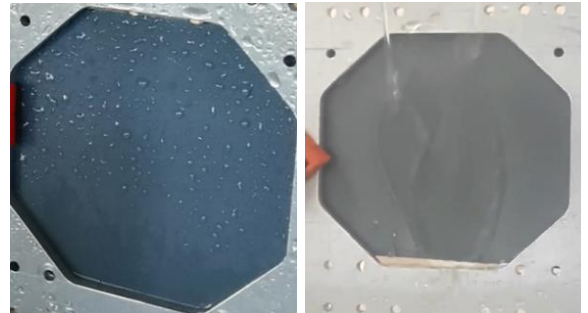


Fig. 10. PVC slab with water drops (left), with water flow (right)

##### B. Measurement and modelling

Measurements in the W band on a wet dielectric slab were carried out with the test bench described in section I. As depicted on Fig. 11, the comparison between the dry and the wet material shows that the reflection coefficients on both sides are very different. The reflection coefficient on the side with water flow is roughly constant (around -10 dB) while on the dry side there is a shift of the resonance frequencies of about 9 GHz.

A cascade of dielectric slabs with parallel faces can be used to model the bumper. The water flow is taken into account as a thin layer made of water with its permittivity described with the single-Debye model as presented in section III.B. Using this very simple approach, the simulated reflection coefficient on the wet side is higher than measurement by about 5 dB, while, on the dry side, the frequency shift is perfectly predicted, as



shown in Fig. 11. A difference of about 2.5 dB between the simulated and measured  $S_{21}$  coefficients was also observed.

The frequency shift of resonances is explained by the sign of the reflection coefficient at the dielectric-to-air interface without ( $\rho_{21}$ , case a) and with water ( $\rho_{23}$ , case b), see Fig. 12.

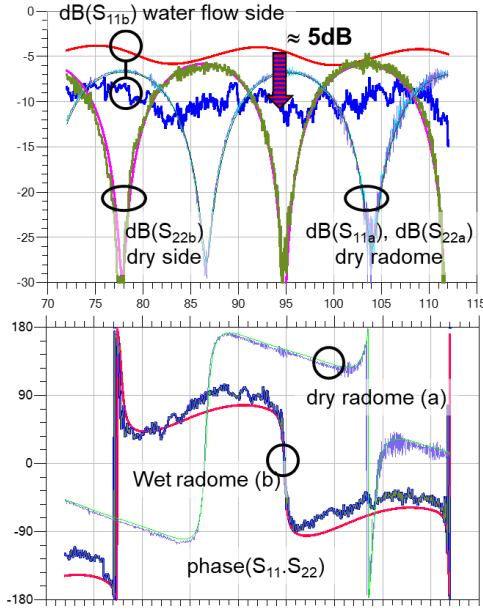


Fig. 11. Water flow effect on the reflexion coefficient (magnitude) of a radome: comparison between model and measurement

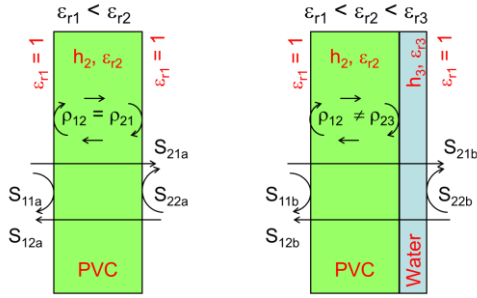


Fig. 12. Reflection coefficient at the dielectric-to-air interface without (case a) and with water (case b)

Because of the high value of water permittivity, the sign of  $\rho_{21}$  is opposite to  $\rho_{23}$  as shown in the following equations:

$$\rho_{21} = \frac{\frac{Z_0}{\sqrt{\epsilon_{r2}}} - Z_0}{\frac{Z_0}{\sqrt{\epsilon_{r2}}} + Z_0} \quad \text{and} \quad \rho_{23} = \frac{\frac{Z_0}{\sqrt{\epsilon_{r2}}} - \frac{Z_0}{\sqrt{\epsilon_{r3}}}}{\frac{Z_0}{\sqrt{\epsilon_{r2}}} + \frac{Z_0}{\sqrt{\epsilon_{r3}}}}, \quad Z_0 = 377 \Omega \quad (2)$$

The water-to-air interface (case b) has low effect on the dry side ( $S_{11b}$ ) because of the high propagation losses into the water layer. However, the maximum magnitude values of the reflection coefficients  $S_{11a}$  and  $S_{11b}$  are almost identical (about -7 to -6 dB) because of the dielectric-to-water interface with a complex reflection coefficient due to the imaginary part of the complex permittivity of water.

A more precise model of the water layer which reflects the wavelets observed on the material surface is now under investigation.

## V. CONCLUSION

Test benches in the Ka, W and J frequency bands using horns and associated lens have been described. Very high measurement quality providing very good performances is validated through a large variety of dielectric slab characterizations for permittivity extraction of solid and non-solid materials. Comparison between measurements and simulations of the 4 S-parameters in magnitude and phase shows the reliability of the technique from millimeter up to the sub-millimeter wave range. The impact on the S-parameters of water drops and water flowing on one side of a dielectric slab has also been investigated and preliminary modelling has been presented.

Further investigations on multilayer slabs and water flow modelling are now underway to study the relationship between rain fall and thickness of water on the bumper and also taking into account the speed of the car in radar applications.

## ACKNOWLEDGMENT

The authors wish to thank numerous colleagues as well as students for their contributions to this work.

## REFERENCES

- [1] M.S. Venkatesh and G.S.V. Raghavan "An overview of dielectric properties measuring techniques" Canadian Biosystems Engineering, Volume 47, 2005
- [2] Le Goff M., Le Bras J.L., Deschamps B., Bourreau D., Peden A. "Ka band quasi optical test bench using focusing horns", *Proc. 29<sup>th</sup> European Microwave Conference*, 1999
- [3] Bourreau D., Péden A., Le Maguer S., "A quasi-optical free-space measurement setup without time-domain gating for material characterization in the W-band", *IEEE Transactions on Instrumentation and Measurement*, december 2006, vol. 55, n° 6, pp. 2022-2026
- [4] Le Bras J.L., Le Goff M., Deschamps B., Peden A., Bourreau D., Toutain S. "Quasi optical circuit measurements method in W band", *ESA workshop*, 1998
- [5] Yaqiang Liu : Doctor of Philosophy "A Novel Free-Space Broadband Dielectric Measurement technique", Waterford Institute of technology (Ireland) May 2014 (Supervisor : Dr Paul O'Leary)
- [6] Liu Y., O'Leary P., "Design of flexible platform for various free-space, broadband dielectric analysis measurement techniques", *IEEE International Workshop on Electromagnetics, Applications and Student Innovation (iWEM)*, 8-10 august 2011
- [7] Kumar Ghodgaonkar D., Khadri N., "Non-destructive and noncontact dielectric measurement methods for low-loss liquids using free space microwave measurement system in 8-12.5 GHz frequency range", *RF and Microwave Conference Proceedings*, 2004
- [8] N. Chen, R. Gourova, O.A Krasnov and A. Yarovoy, "The Influence of the Water-covered Dielectric Radome on 77GHz Automotive Radar Signals", *Proc. of the 14th European Radar Conference 11-13 Oct 2017*, Nuremberg, Germany
- [9] P.F. Goldsmith "Quasi-optical techniques" *Proceedings of the IEEE*, Vol. 80, Issue: 11, Nov 1992
- [10] Garcia-Ruiz I., Aviles-Castro C. D., Jardon-Aguilar H., Guerra-Vargas J., "On the measurement of the complex permittivity of layers embedded in a multilayer dielectric material with the use of the free-space method", *Microwave and Optical technology letters*, vol 33 n°6, june 20 2012
- [11] A. Arage, W. M. Steffens, G. Kuehnle, and R. Jakoby, "Effects of water and ice layer on automotive radar" in *Proc. of the German Microwave Conf*, 2006.
- [12] Sinan Hasirlioglu Andreas Rienen "A General Approach for Simulating Rain Effects on Sensor Data in Real and Virtual Environments", *IEEE Transactions on Intelligent Vehicles*, 19 December 2019.